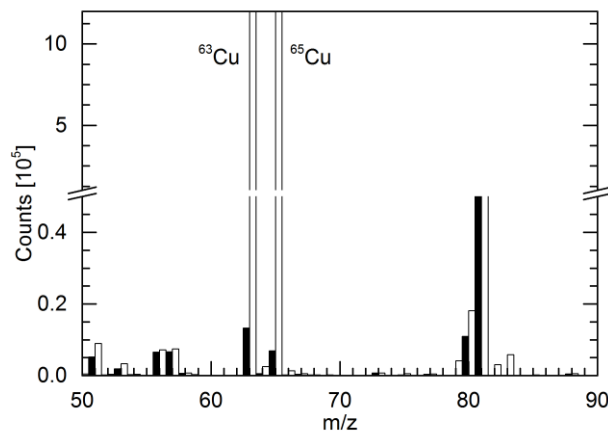


SUPPORTING INFORMATION

Copper Oxide as Efficient Catalyst for Oxidative Dehydrogenation of Alcohols with Air

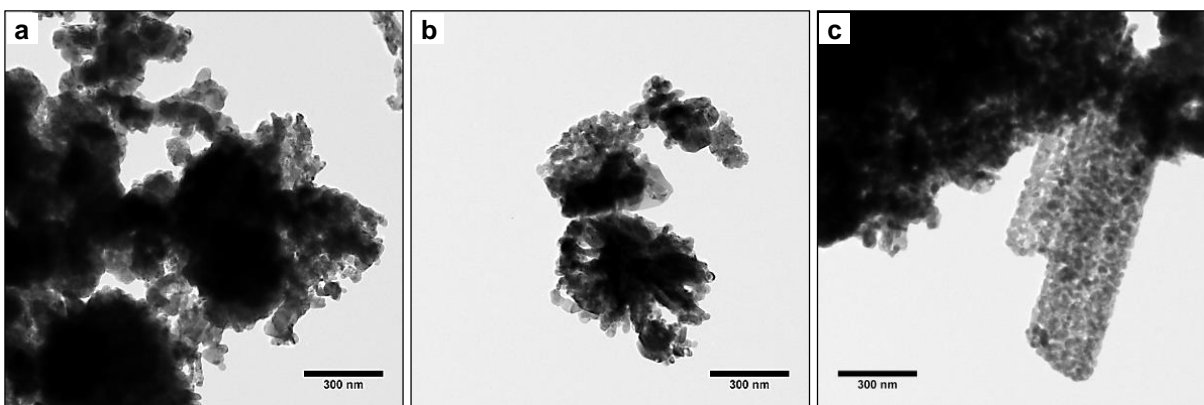
Raju Poreddy, Christian Engelbrekt and Anders Riisager*

Inductively coupled plasma mass spectrometry (ICP-MS)



SI Fig. 1. ICP-MS of dissolved CAPS-CuO (white) and filtered solution after reaction for 24 h with CAPS-CuO catalyst (black).

Transmission electron microscopy

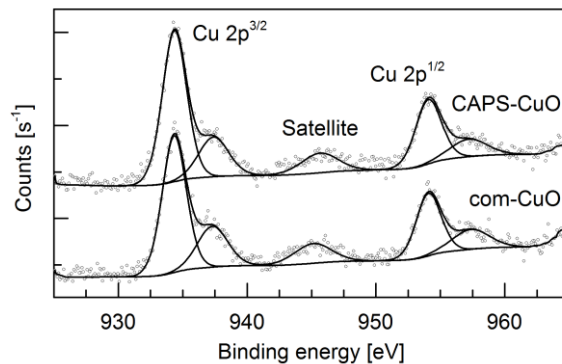


SI Fig. 2. TEM micrographs of as-received commercial CuO (com-CuO).

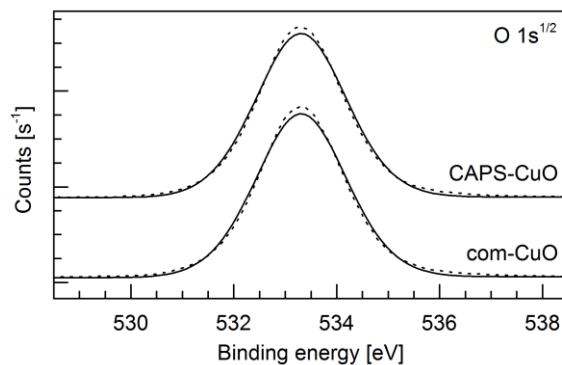
SI Table 1. Observed lattice spacings derived from the FFTs shown in Fig. 3 compared with calculated values.

| | | CAPS-CuO | | | MES-CuO | | |
|---------|-----------------|----------|------------------|------------------|-----------------|------------------|------------------|
| | | (hkl) | d_{obs} | d_{cal} | (hkl) | d_{obs} | d_{cal} |
| Fig. 3b | (020) | | 1.70 Å | 1.71 Å | (3 $\bar{1}1$) | 1.33 Å | 1.30 Å |
| | (200) | | 2.31 Å | 2.31 Å | (31 $\bar{1}$) | 1.42 Å | 1.41 Å |
| | (110) | | 2.73 Å | 2.75 Å | (0 $\bar{2}2$) | 1.45 Å | 1.42 Å |
| | ($\bar{1}10$) | | 2.78 Å | 2.75 Å | (200) | 2.33 | 2.31 Å |
| Fig. 3d | (020) | | 1.72 Å | 1.71 Å | (1 $\bar{1}1$) | 2.35 | 2.32 Å |
| | (200) | | 2.33 Å | 2.31 Å | (11 $\bar{1}$) | 2.56 Å | 2.52 Å |
| | (110) | | 2.73 Å | 2.75 Å | (3 $\bar{1}1$) | 1.33 Å | 1.30 Å |
| | ($\bar{1}10$) | | 2.80 Å | 2.75 Å | (200) | 2.30 Å | 2.31 Å |

X-ray photoelectron spectroscopy (XPS)

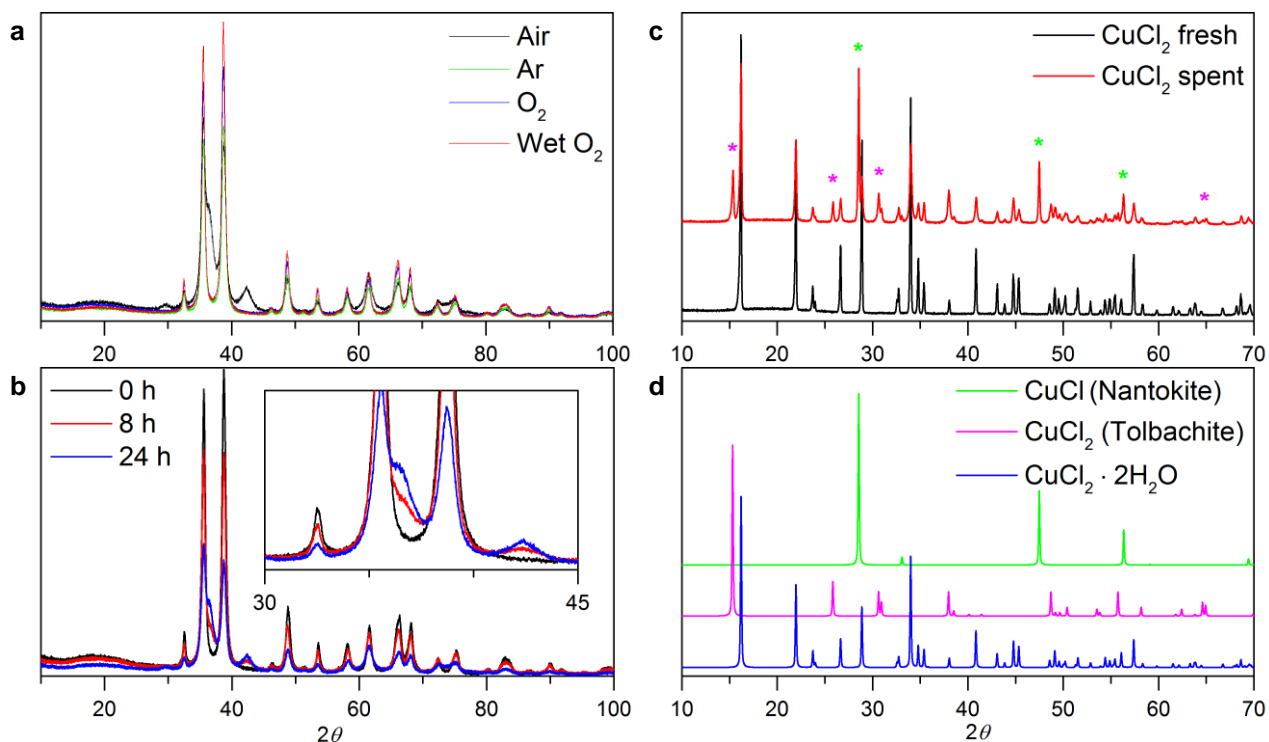


SI Fig. 3. XPS at the Cu 2p transition of CAPS-CuO (top) and MES-CuO (bottom).



SI Fig. 4. XPS at the O1s transition of CAPS-CuO (top) and com-CuO (bottom).

X-ray powder diffraction (XRD)



SI Fig. 5. XRD patterns of CAPS-CuO (a) after 24 h reaction in different atmospheres and (b) at different times during reaction. Inset in (b) shows a magnified view of the predominant Cu₂O peaks at 36.5° and 42.4°, respectively. The XRD patterns in (c) show the structural changes of CuCl₂ when used as catalyst. Reference patterns in (d) support that both dehydration and significant reduction to CuCl occurs.

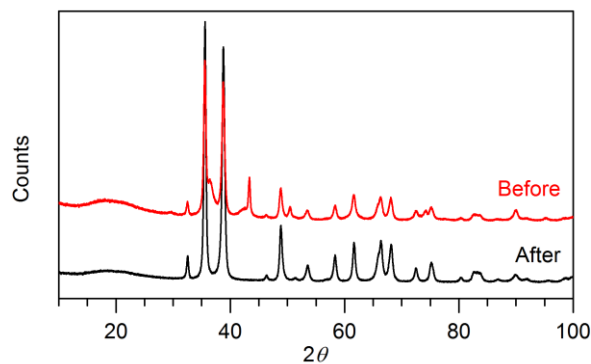
Rietveld refinement parameters

The crystal structures of fresh and spent CAPS-CuO and MES-CuO were refined by WINPOW (a local variation of LHMP). The Rietveld refinement for anatacamite was carried out by refining in a 2θ range from 20° (fresh) and 10° (spent) to 100° in steps of 0.02°. No atomic coordinates were refined. A Voigt profile function and a Chebyshev background polynomial were applied in all refinements. Crystallographic data and refinement summary are given in SI Table 2 and the refined patterns are shown in Fig. 1.

SI Table 2. Crystallographic data and refinement summary for the as-synthesized and spent CuO catalysts.

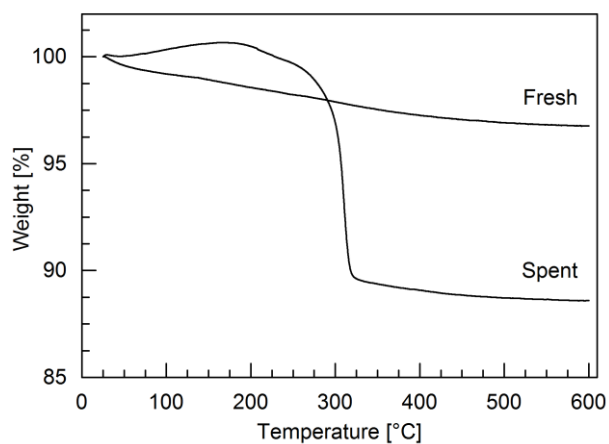
| Sample | CAPS-CuO | | CAPS-CuO | | | MES-CuO | | |
|------------------------------------|------------|------------|------------|-------------------|-----------|------------|-------------------|-----------|
| | (Fresh) | (Fresh) | (Spent) | | | (Spent) | | |
| Formula | CuO | CuO | CuO | Cu ₂ O | Cu | CuO | Cu ₂ O | Cu |
| Formula mass (g/mol) | 79.55 | 79.55 | 79.55 | 143.1 | 63.55 | 79.55 | 143.1 | 63.55 |
| Crystal system | Monoclinic | Monoclinic | Monoclinic | Cubic | Cubic | Monoclinic | Cubic | Cubic |
| Space group | C 1 c 1 | C 1 c 1 | C 1 c 1 | P n -3 m Z | F m -3 m | C 1 c 1 | P n -3 m Z | F m -3 m |
| <i>a</i> (Å) | 4.6817(2) | 4.6833(2) | 4.6930(4) | 4.2596(3) | 3.5938(1) | 4.730(2) | 4.2631(2) | 3.6151(1) |
| <i>b</i> (Å) | 3.4175(2) | 3.4170(2) | 3.4260(3) | 4.2596(3) | 3.5938(1) | 3.415(1) | 4.2631(2) | 3.6151(1) |
| <i>c</i> (Å) | 5.1317(3) | 5.1302(3) | 5.1240(5) | 4.2596(3) | 3.5938(1) | 5.022(2) | 4.2631(2) | 3.6151(1) |
| <i>α</i> (°) | 90 | 90 | 90 | 90 | 90 | 90 | 90 | 90 |
| <i>β</i> (°) | 99.266(2) | 99.275(2) | 99.332(5) | 90 | 90 | 99.39(2) | 90 | 90 |
| <i>γ</i> (°) | 90 | 90 | 90 | 90 | 90 | 90 | 90 | 90 |
| <i>V</i> (Å³) | 81.04(1) | 81.03(1) | 81.29(2) | 77.29(2) | 46.42(5) | 80.04(9) | 77.48(1) | 47.245(5) |
| <i>Z</i> | 4 | 4 | 4 | 2 | 4 | 4 | 2 | 4 |
| <i>ρ</i> (g/cm³) | 6.519 | 6.520 | 6.498 | 6.148 | 9.092 | 6.600 | 6.133 | 8.933 |
| Voigt particle size (Å) | 175(0) | 188(1) | - | - | - | - | - | - |
| Composition (wt%) | | | 77.6(3) | 21.1(1) | 1.29(4) | 6.8(1) | 77.6(3) | 15.60(8) |
| No. of parameters | 12 | 12 | | 27 | | | 24 | |
| <i>R_{wp}</i> (%) | 2.49 | 2.81 | | 4.93 | | | 5.50 | |
| <i>χ</i>² | 0.35 | 0.48 | | 2.30 | | | 2.82 | |
| <i>R_p</i> (%) | 1.80 | 2.08 | | 3.50 | | | 4.14 | |
| No. of Bragg reflections | 46 | 46 | 46 | 12 | 5 | 42 | 12 | 5 |
| <i>R_B</i> (%) | 1.25 | 1.51 | 2.49 | 1.54 | 0.83 | 1.54 | 1.70 | 1.79 |

XRD of spent and regenerated CAPS-CuO



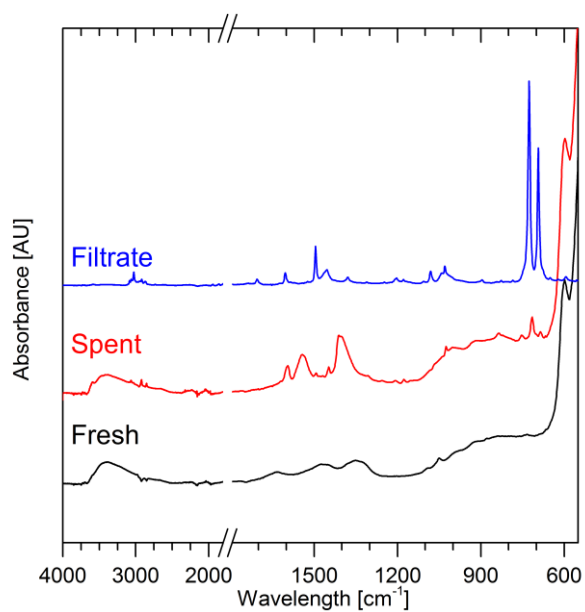
SI Fig. 6. XRD of CAPS-CuO before and after the thermal treatment.

Thermogravimetric analysis (TGA)



SI Fig. 7. TGA of fresh and spent CAPS-CuO with a heating rate of 10 °C/min.

Attenuated total reflectance Fourier transformed infrared spectroscopy (ATR-FTIR)



SI Fig. 8. ATR-FTIR spectra of fresh CAPS-CuO (black), spent CAPS-CuO after fourth reaction run without regeneration (red) and the reaction filtrate (blue).